molbank

MDPI

SUPPLEMENTARY MATERIALS

Short Note

(*E*)-4-(3-(3-(4-Methoxyphenyl)acryloyl)phenoxy)butyl 2-Hydroxybenzoate

Ihsan Ikhtiarudin [1,*], Rahma Dona [1], Neni Frimayanti [1], Rahayu Utami [1], Emma Susanti [1], Mentari Mentari [1], Nurmaida Nurmaida [1], Nesa Agistia [1], Noval Herfindo [2,3], and Adel Zamri [3]

[1] Department of Pharmacy, Sekolah Tinggi Ilmu Farmasi (STIFAR) Riau, Pekanbaru, 28293, Indonesia; rahmadona@stifar-riau.ac.id (R.D.); nenifrimayanti@gmail.com (N.F.); rahayuutami@stifar-riau.ac.id (R.U.); emmasusanti@stifar-riau.ac.id (E.S.); nrmaida12@gmail.com (N.N.); 15mentari@stifar-riau.ac.id (M.M.); nesaagistia@stifar-riau.ac.id (N.A.).

[2] Department of Biomedical Engineering, Faculty of Engineering, King Mongkut's Institute of Technology Ladkrabang, Bangkok 10520, Thailand; novalherfindo@gmail.com (N.H.).

[3] Department of Chemistry, Faculty of Mathematics and Natural Sciences, Universitas Riau, Pekanbaru, 28293, Indonesia; adel.zamri@lecturer.unri.ac.id (A.Z).

* Correspondence: ihsanikhtiarudin@stifar-riau.ac.id

Figure S1. The clear yellow crystal of the title compound (hybrid compound)

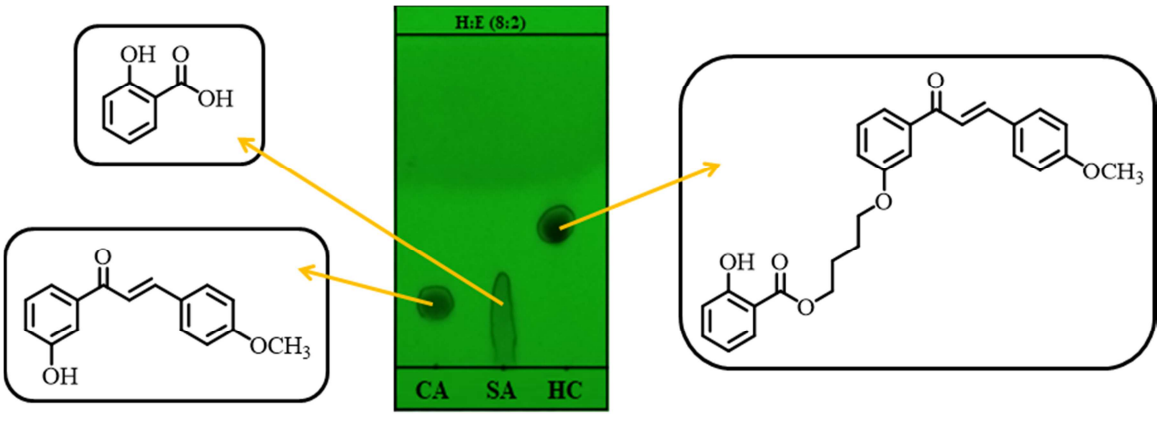

Figure S2. TLC chromatogram of hybrid compound (HC) compared to chalcone analog (CA) and salicylic acid (SA) as starting materials under UV lamp, 254 nm. H = *n*-hexane and E = ethyl acetate

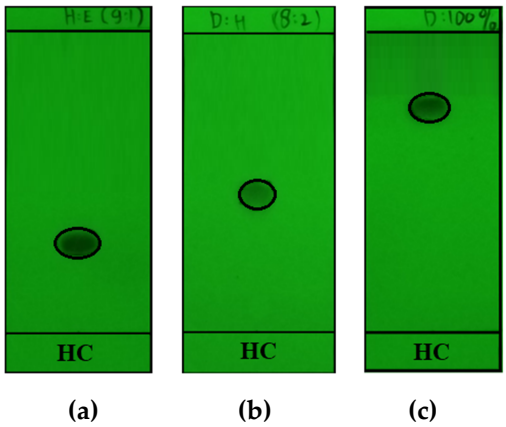

Figure S3. The result of TLC analysis of hybrid compound using various mobile phases: (a) *n*-hexane:ethyl acetate (9:1), (b) DCM: *n*-hexane (8:2), (c) D100% = DCM 100%

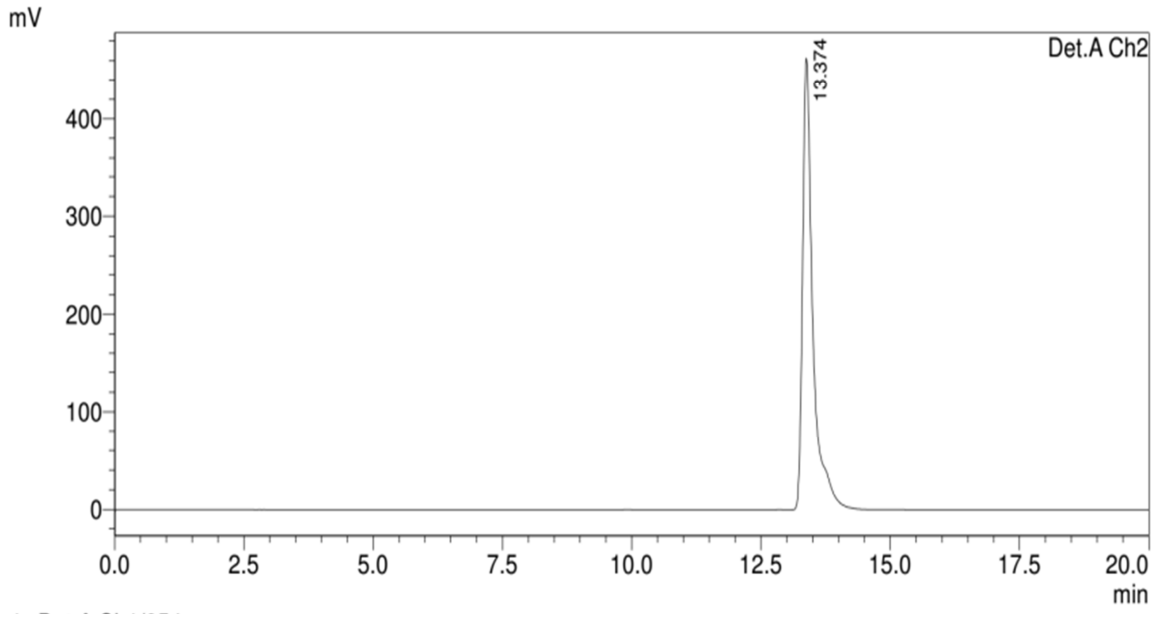

Figure S4. HPLC chromatogram of hybrid compound, analysis was performed using reverse phase column Shim-Pack VP-ODS (150 x 4.6 mm) with gradient elusion method using water and acetonitrile (HPLC grade) as mobile phase for 20 minutes with flow rate 1 ml/minute

Table S1. Mobile phase composition for HPLC analysis of hybrid compound

[33] Minutes	Mobile phases	
	water	acetonitrile
1	30	70
4	30	70
12	10	90
15	10	90
19	10	90
20	**Stop**	

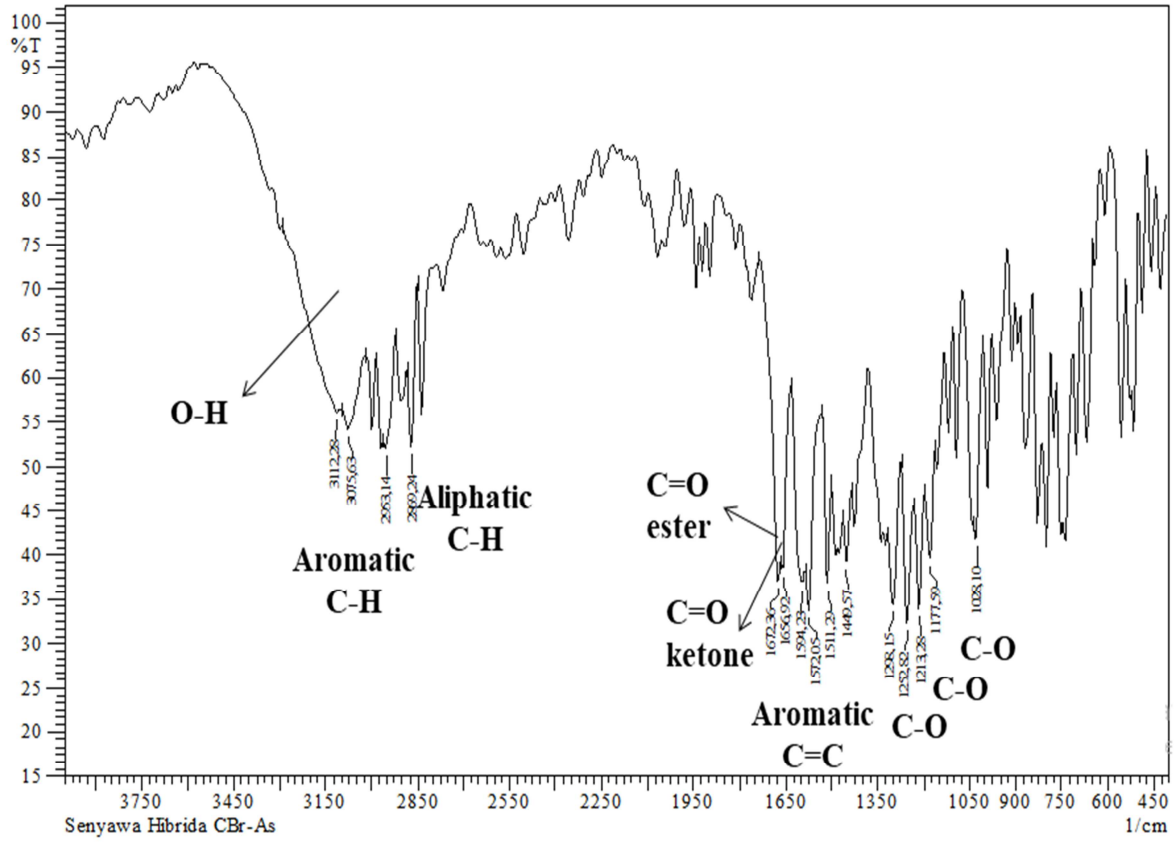

Figure S5. The FTIR spectra of hybrid compound

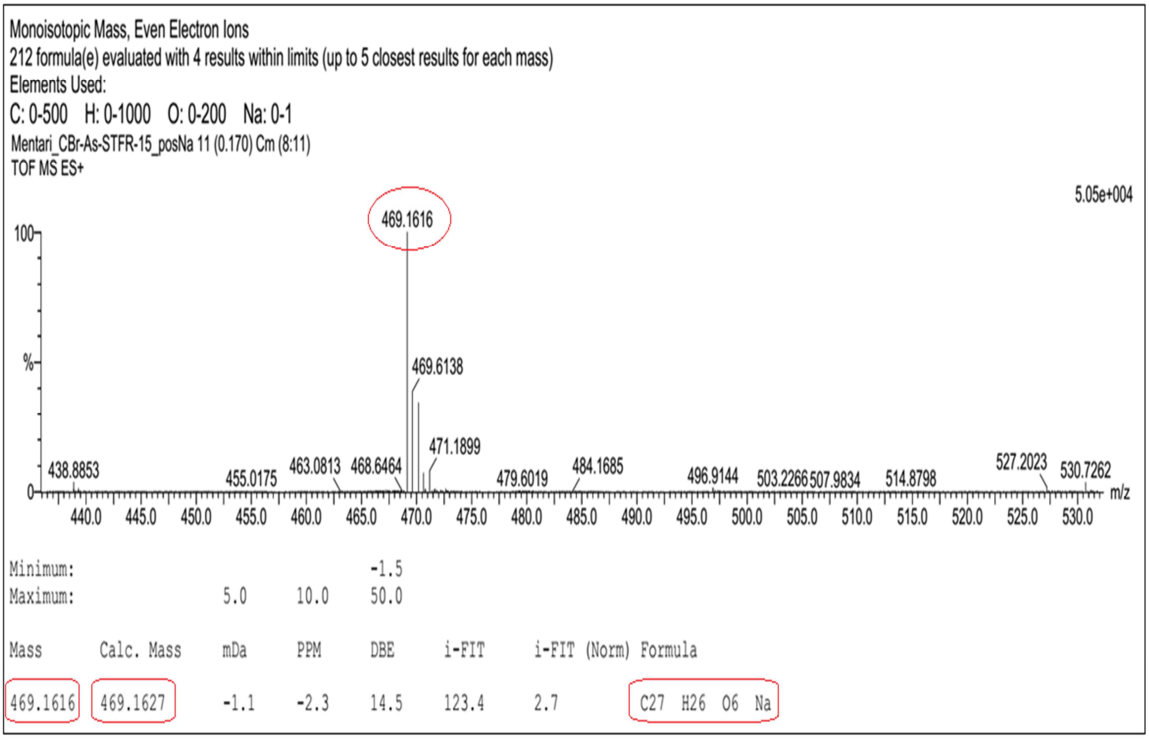

Figure S6. The HRMS spectra of hybrid compound

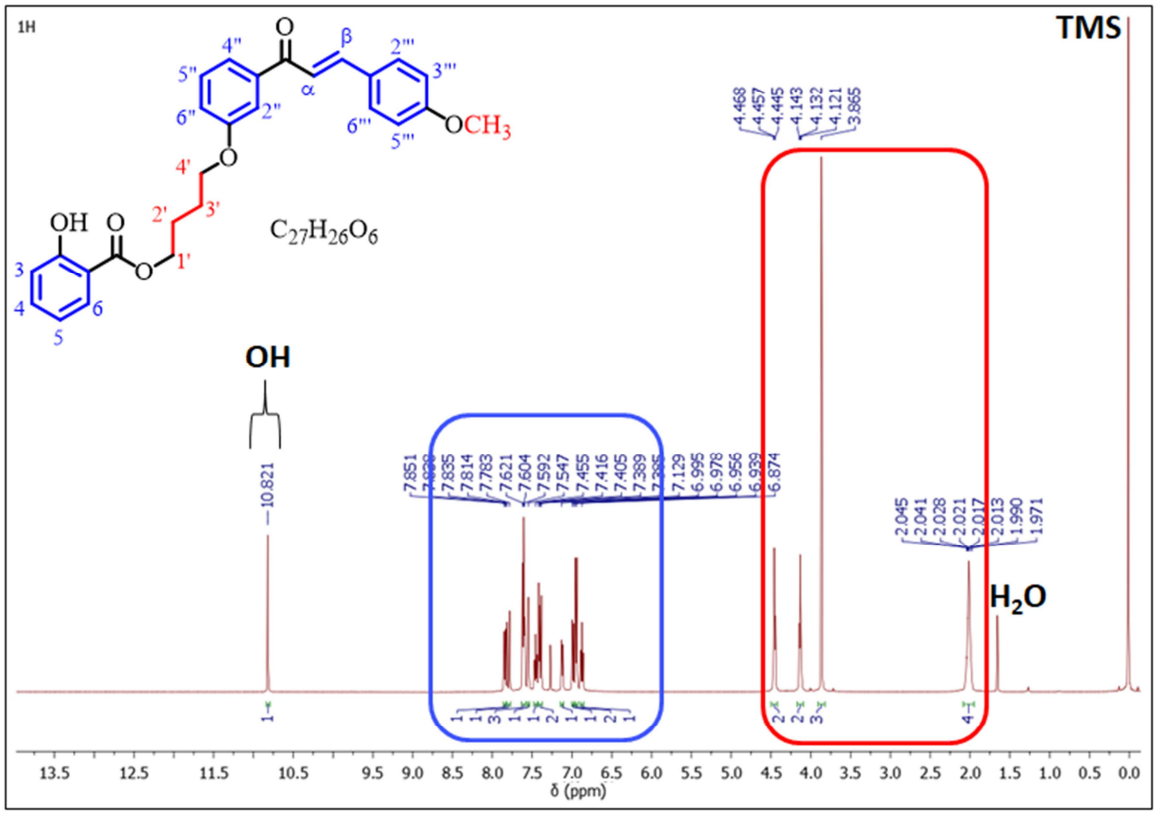

Figure S7. The ^{1}H NMR spectra of hybrid compound in $CDCl_3$ (500 MHz)

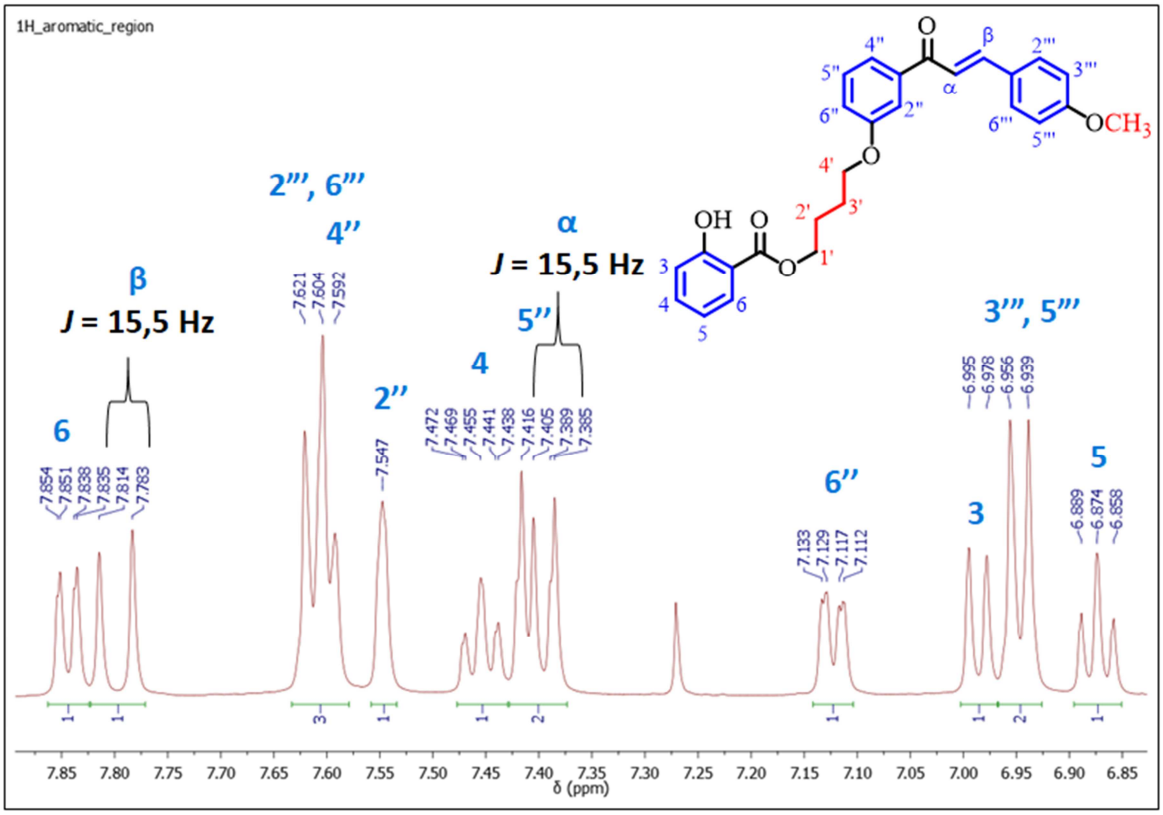

Figure S8. The ^{1}H NMR spectra of hybrid compound in $CDCl_3$ (500 MHz), expansion in aromatic region

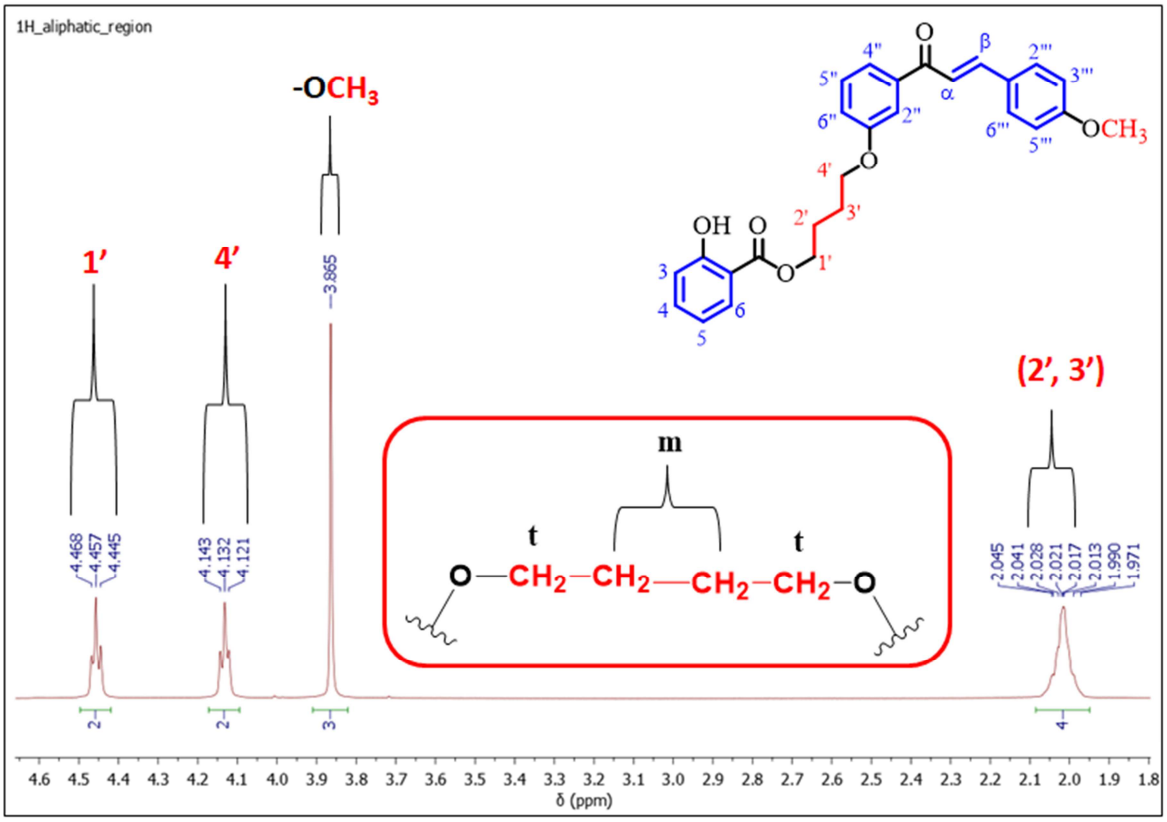

Figure S9 The ^{1}H NMR spectra of hybrid compound in $CDCl_3$ (500 MHz), expansion in aliphatic region

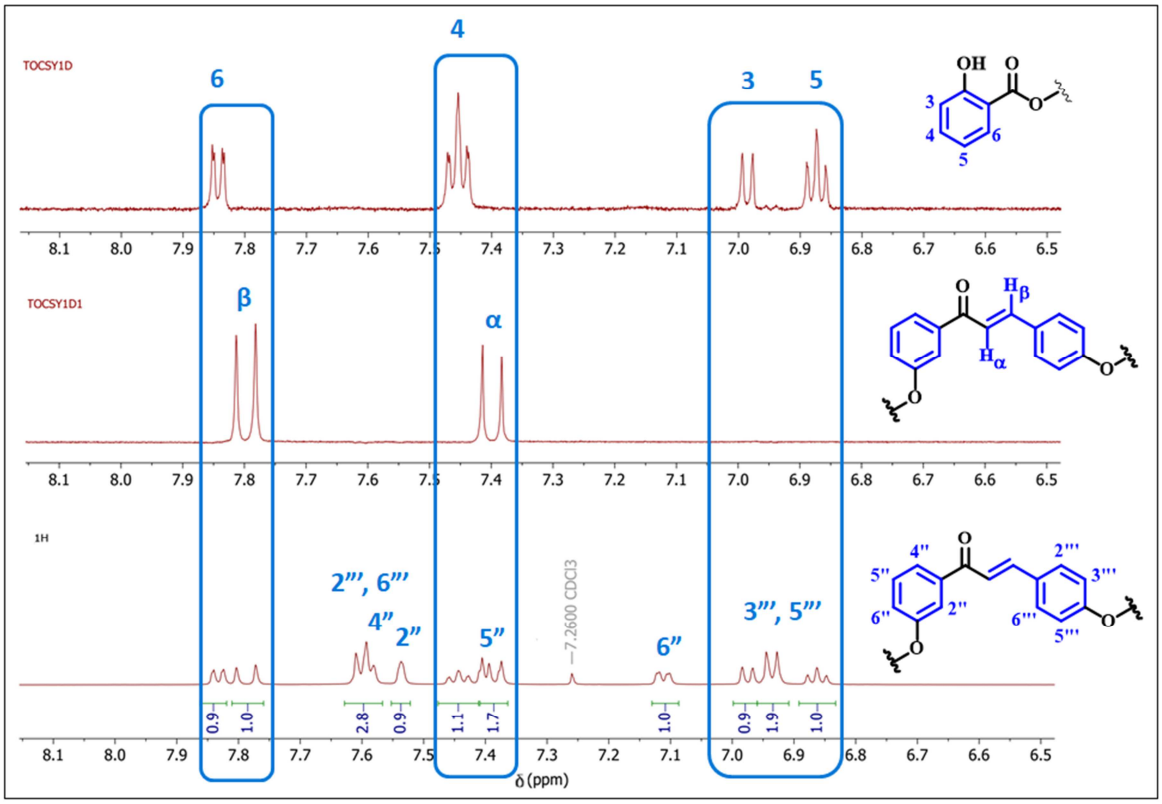

Figure S10. The 1D TOCSY spectra of aromatic region of hybrid compound in $CDCl_3$ (500 MHz)

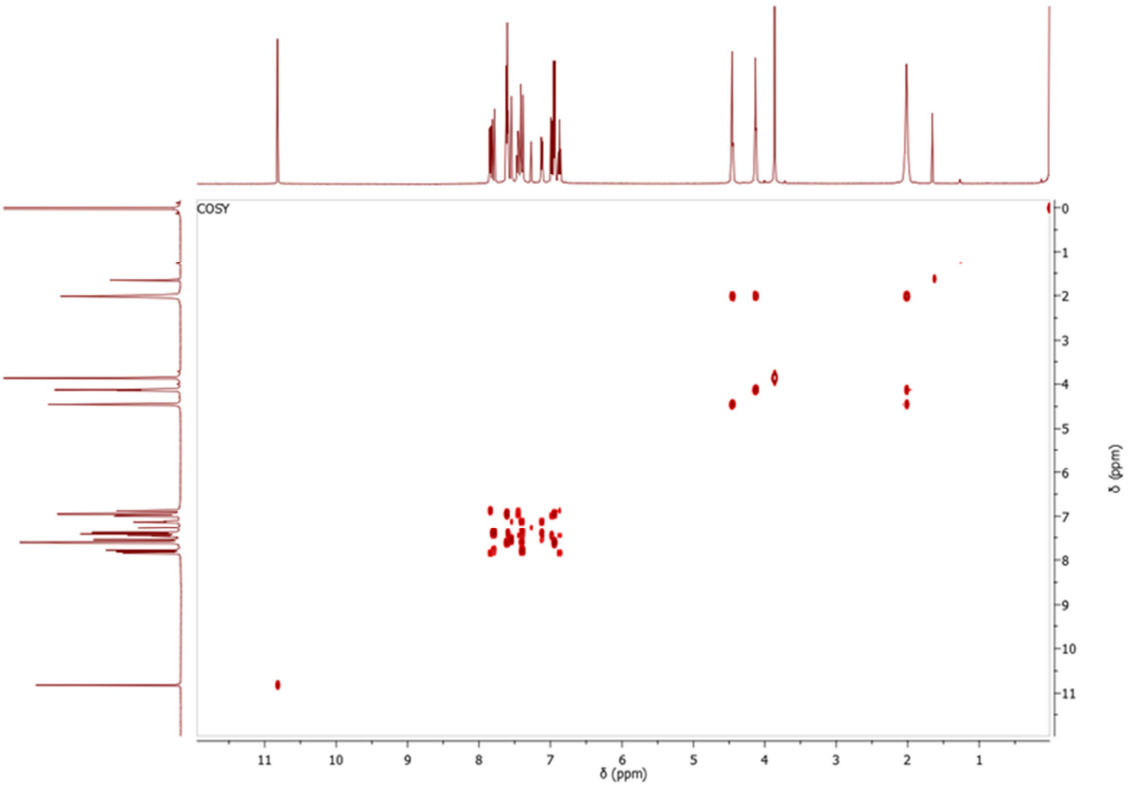

Figure S11. The COSY spectra of hybrid compound in $CDCl_3$ (500 MHz)

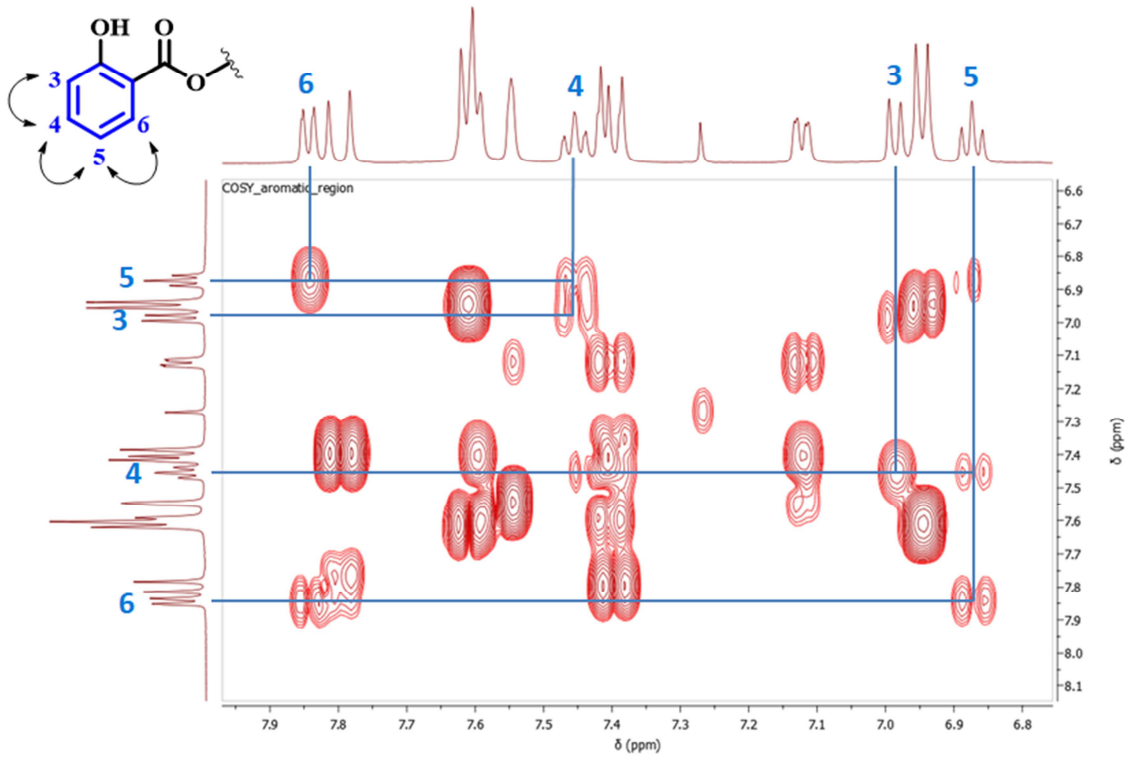

Figure S12. The COSY spectra of hybrid compound in $CDCl_3$ (500 MHz), expansion in R aromatic region

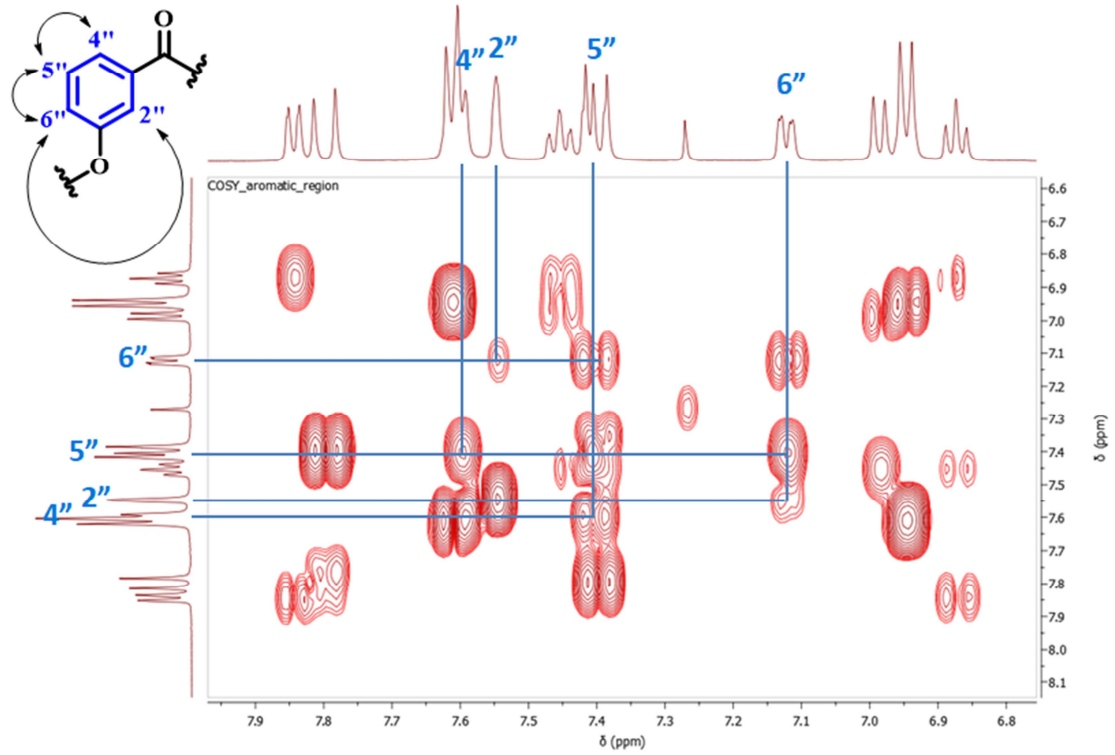

Figure S13. The COSY spectra of hybrid compound in $CDCl_3$ (500 MHz), expansion in R″ aromatic region

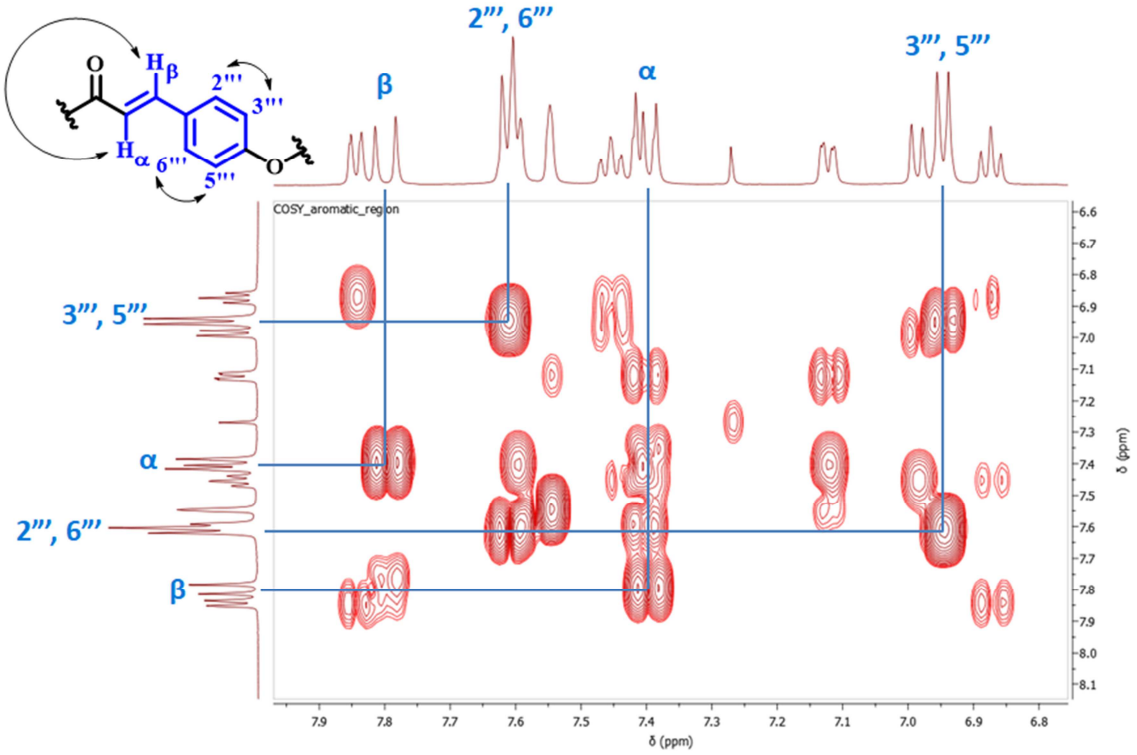

Figure S14. The COSY spectra of hybrid compound in $CDCl_3$ (500 MHz), expansion in R‴ aromatic region

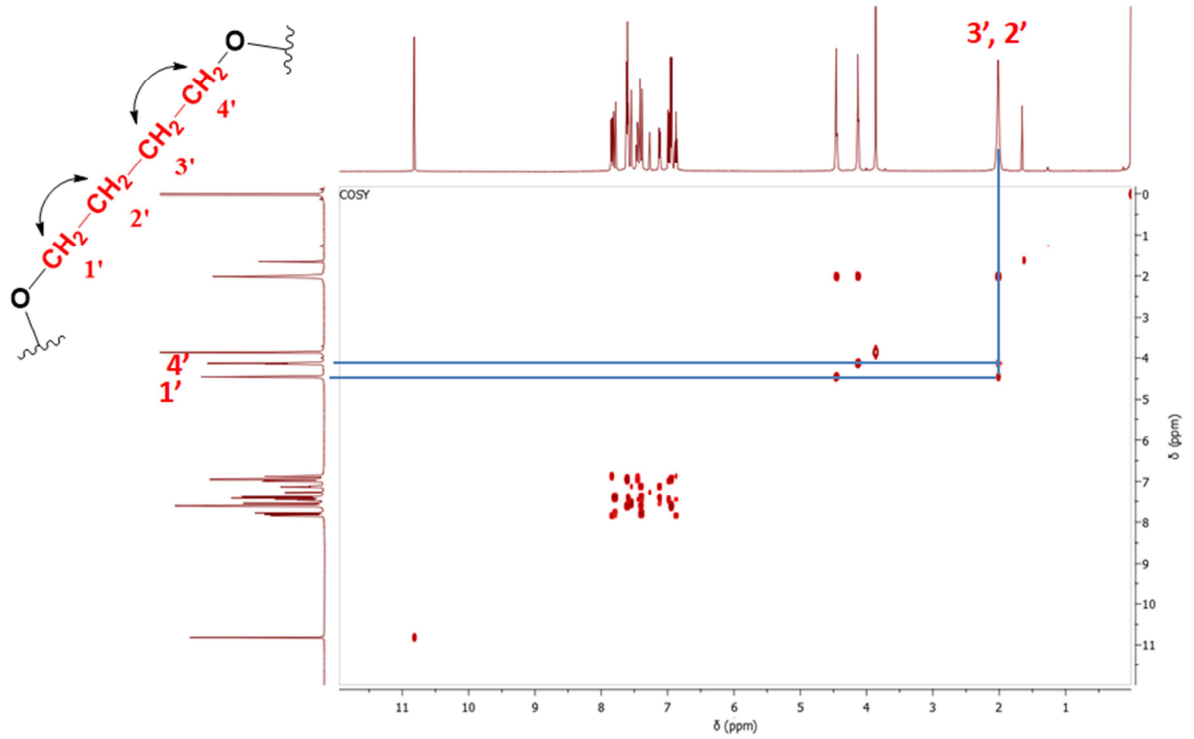

Figure S15. The COSY spectra of hybrid compound in $CDCl_3$ (500 MHz), expansion in aliphatic region

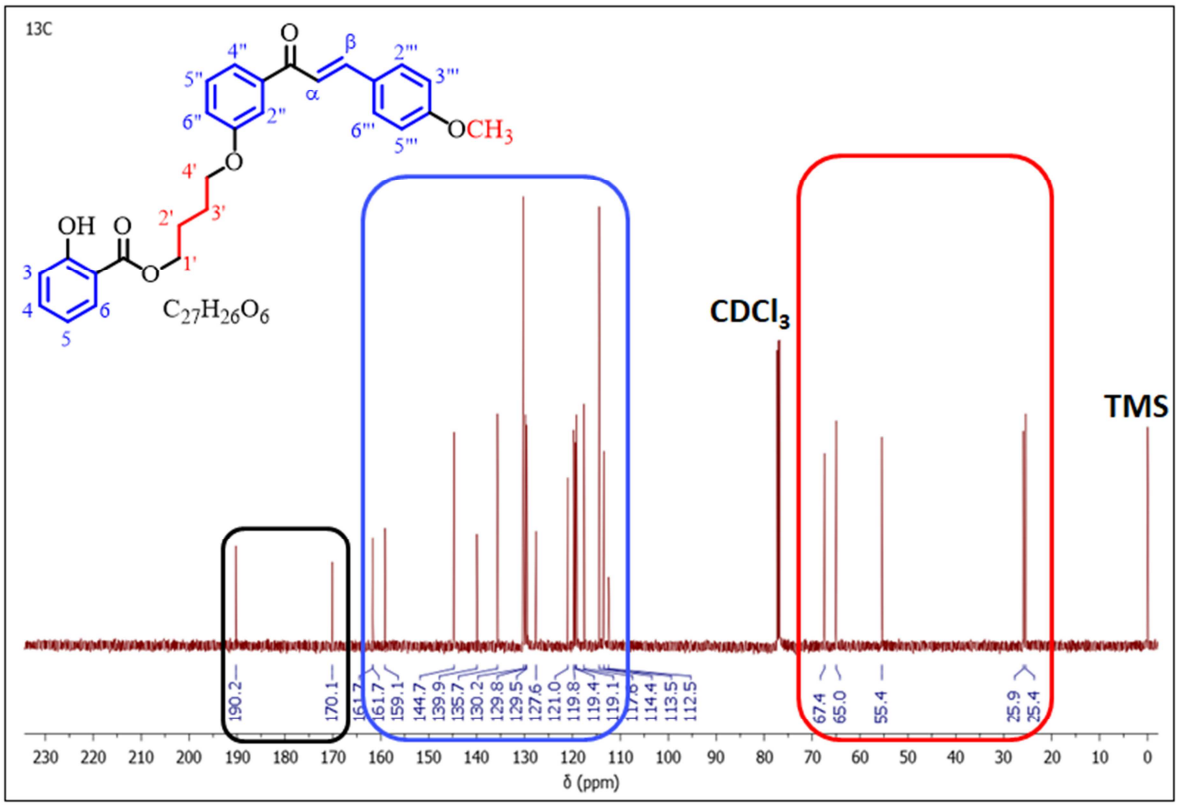

Figure S16. The ^{13}C NMR spectra of hybrid compound in $CDCl_3$ (125 MHz)

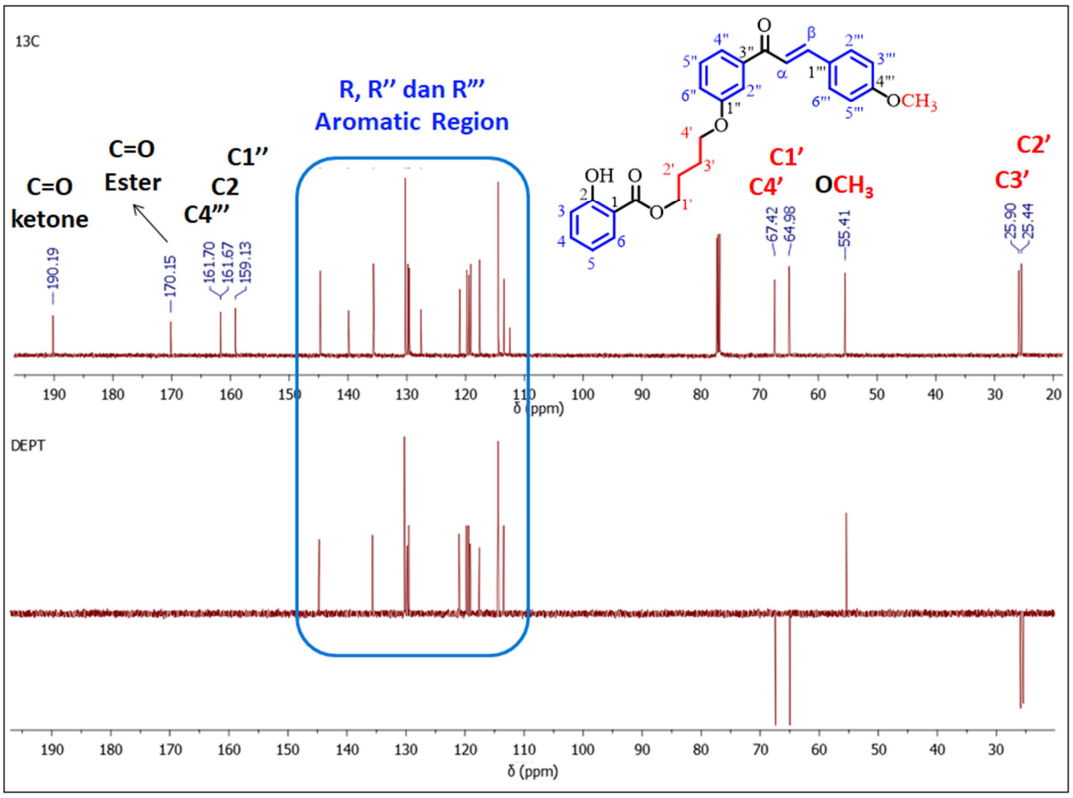

Figure S17. The Overlay of ^{13}C NMR and DEPT-135 spectra of hybrid compound in $CDCl_3$ (125 MHz)

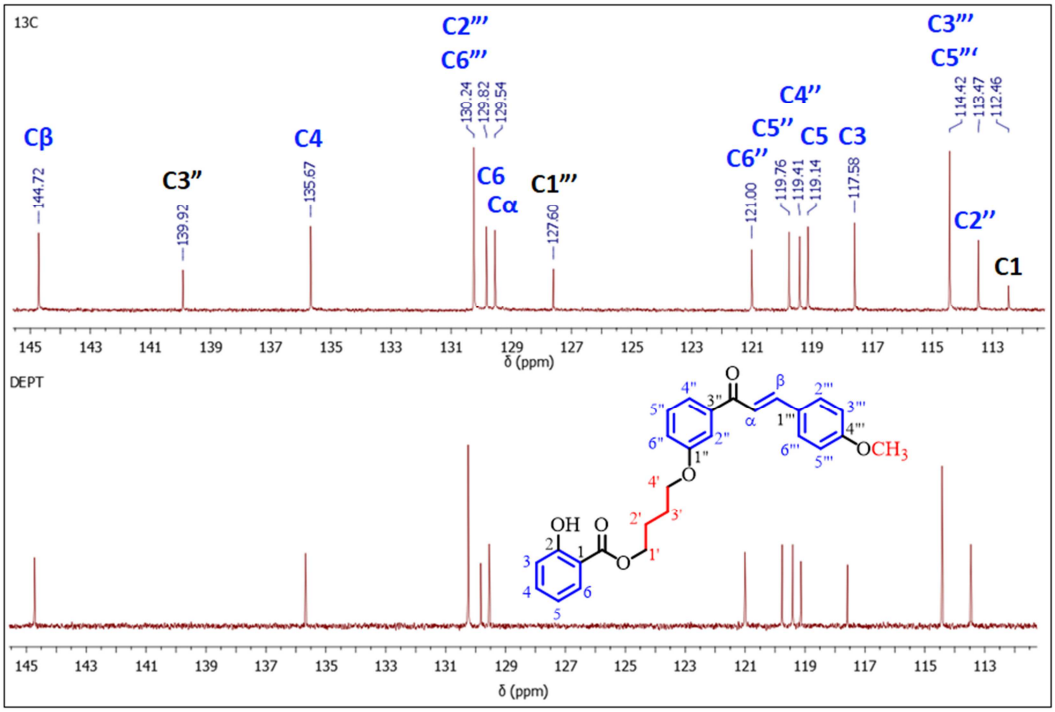

Figure S18. The overlay of ^{13}C NMR and DEPT-135 spectra of hybrid compound in $CDCl_3$ (125 MHz), expansion in aromatic region

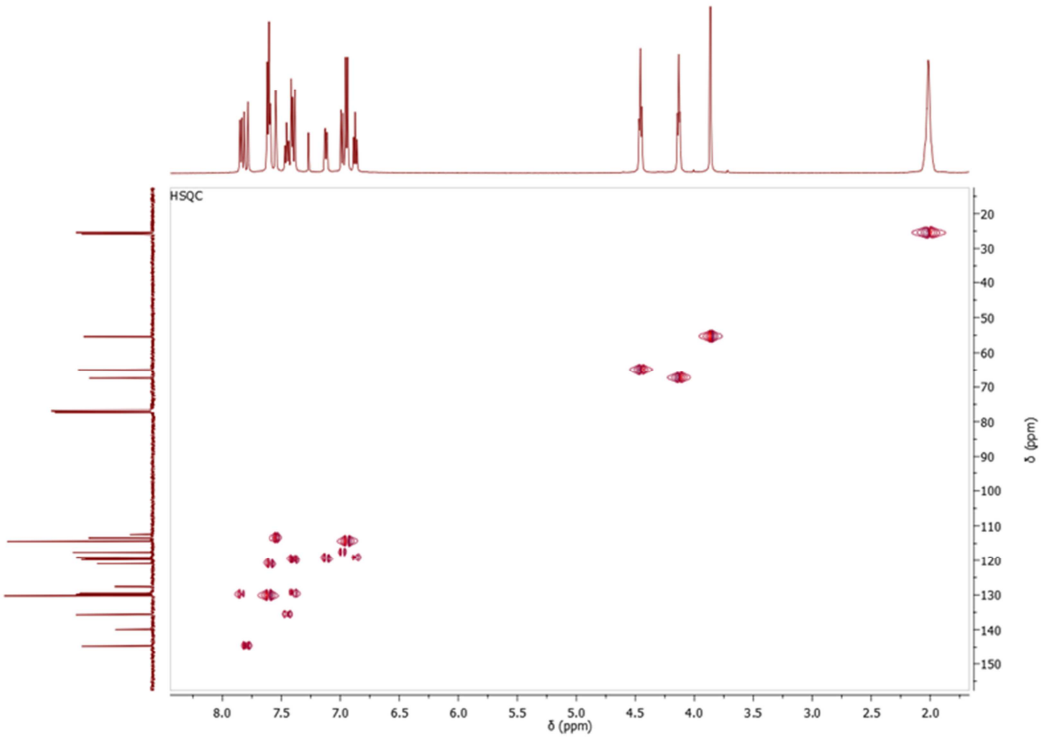

Figure S19. The HSQC spectra of hybrid compound in $CDCl_3$ (500 MHz), expansion in aromatic region

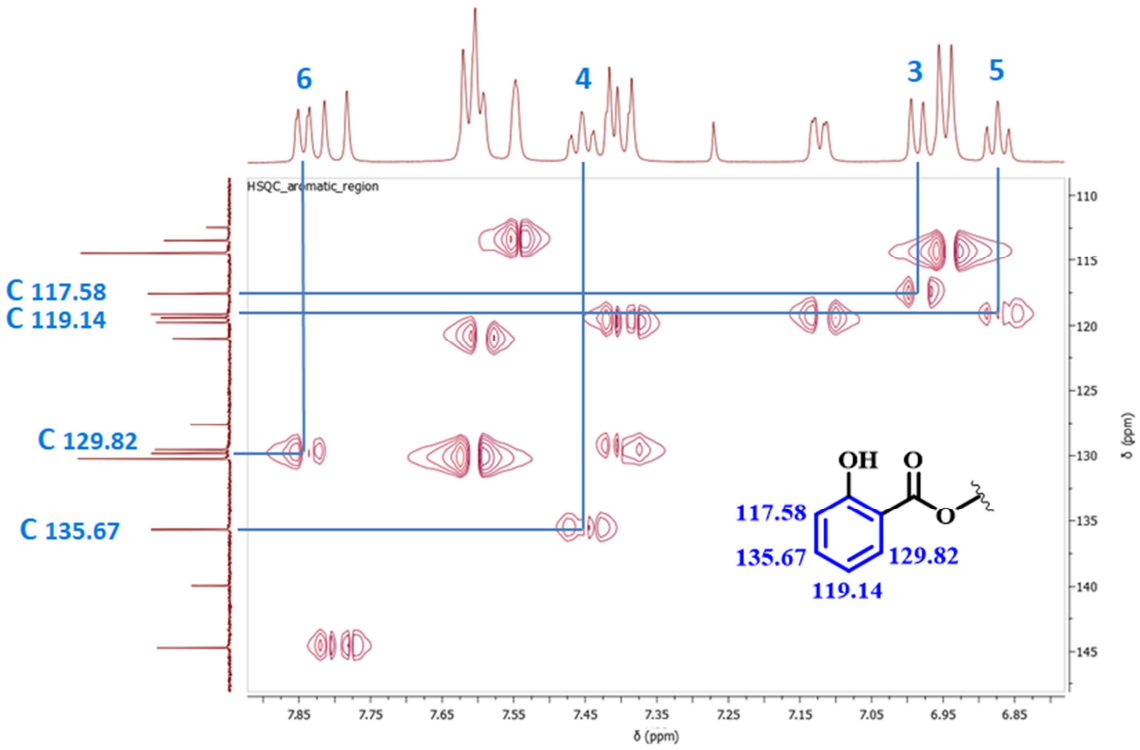

Figure S20. The ^{1}H-^{13}C correlations of R aromatic region in HSQC spectra of hybrid compound in $CDCl_3$

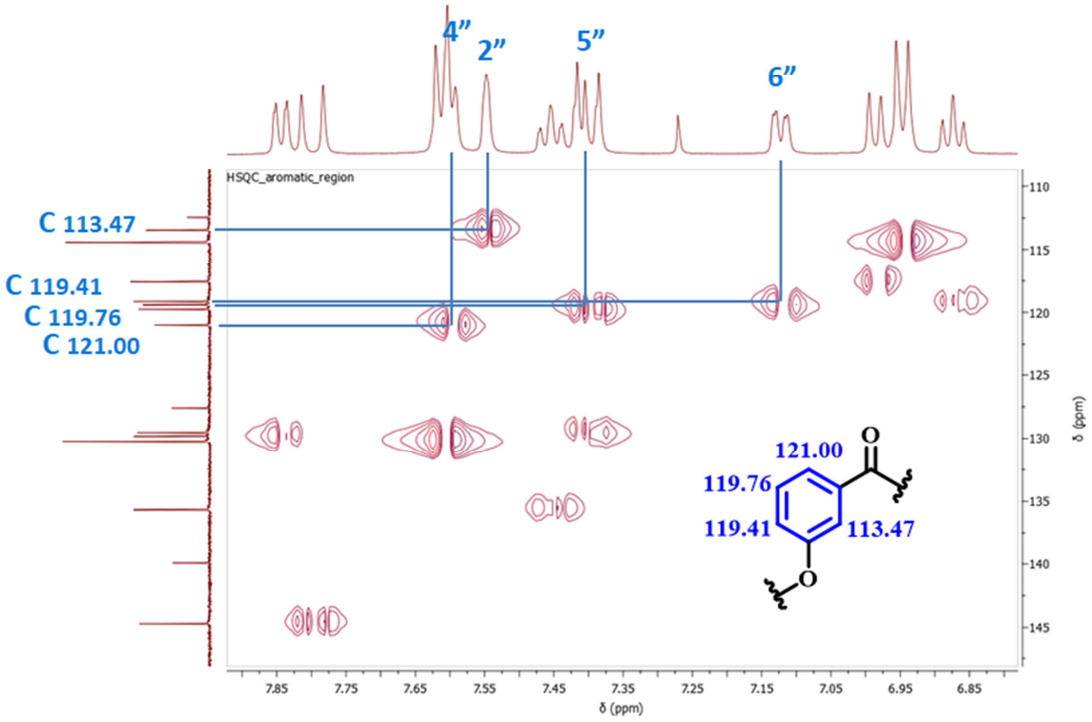

Figure S21. The ^{1}H-^{13}C correlations of R'' aromatic region in HSQC spectra of hybrid compound in $CDCl_3$

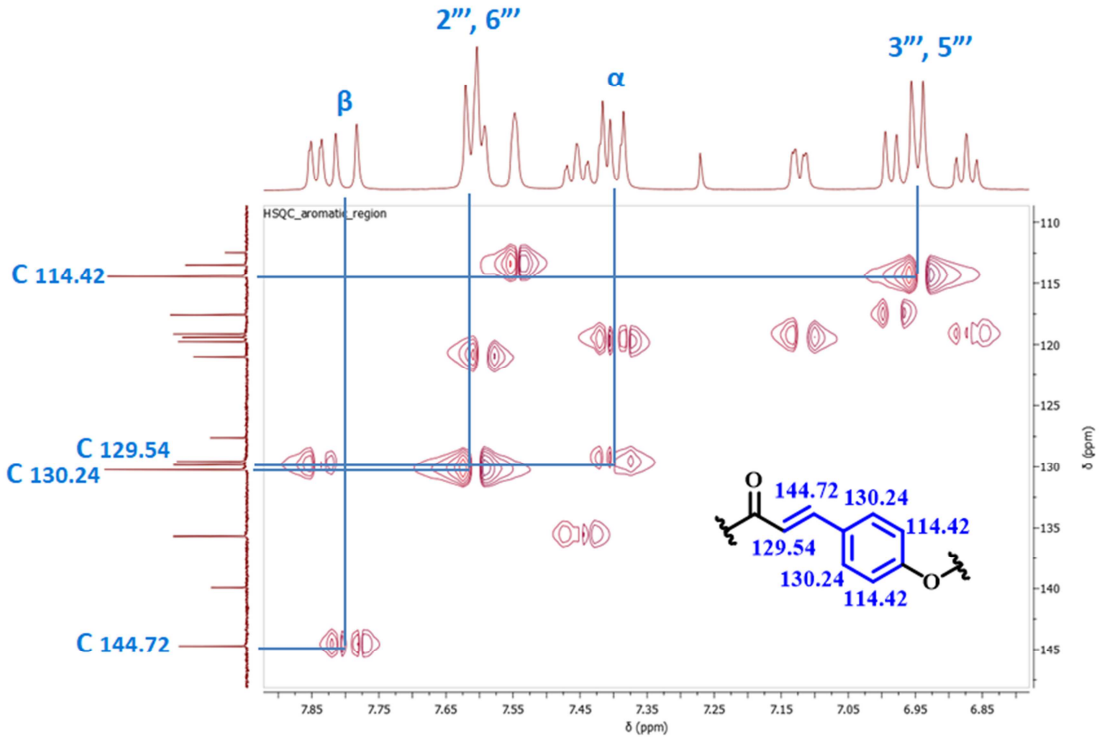

Figure S22. The^{1}H-^{13}C correlations of R''' aromatic region in HSQC spectra of hybrid compound in $CDCl_3$

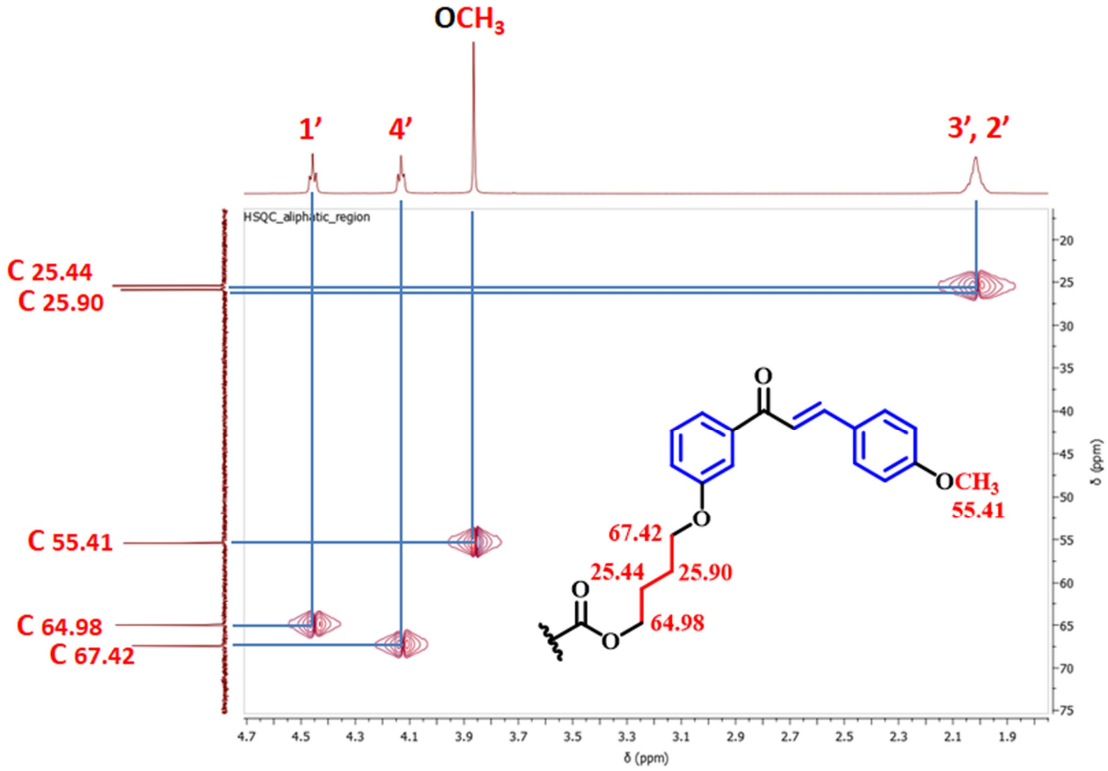

Figure S23. The ^{1}H-^{13}C correlations of aliphatic region in HSQC spectra of hybrid compound in $CDCl_3$ (500 MHz)

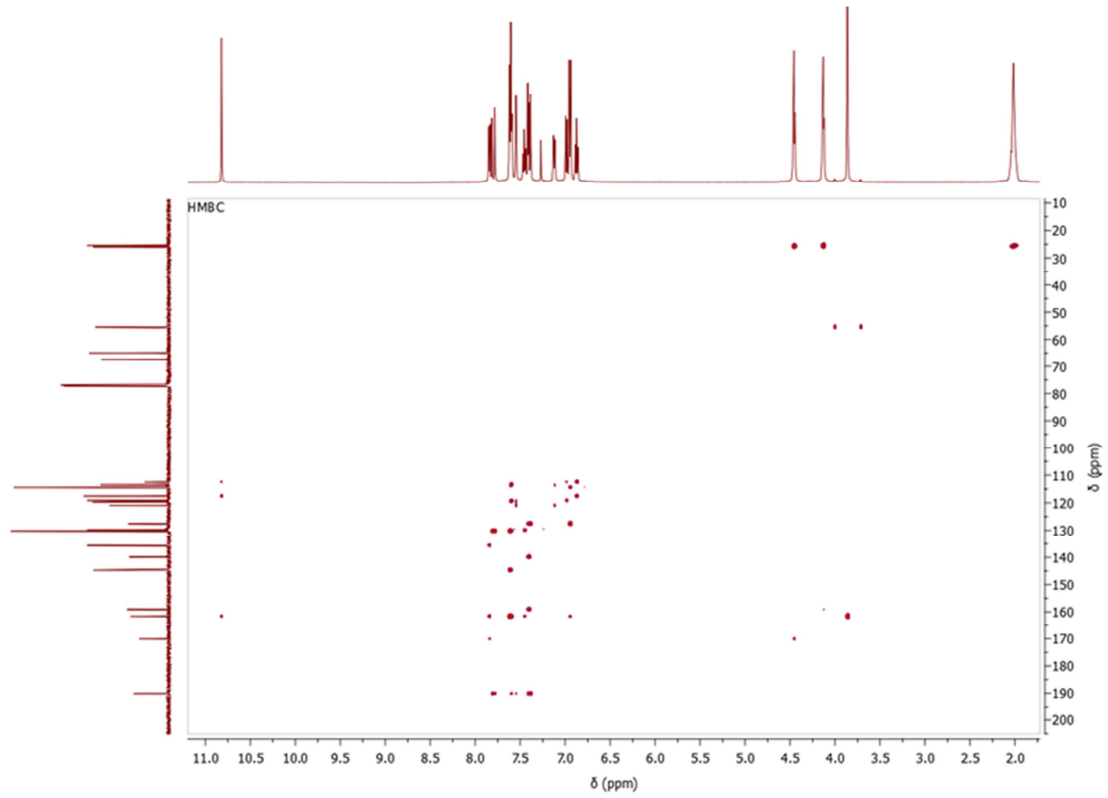

Figure S24. The HMBC spectra of hybrid compound in $CDCl_3$

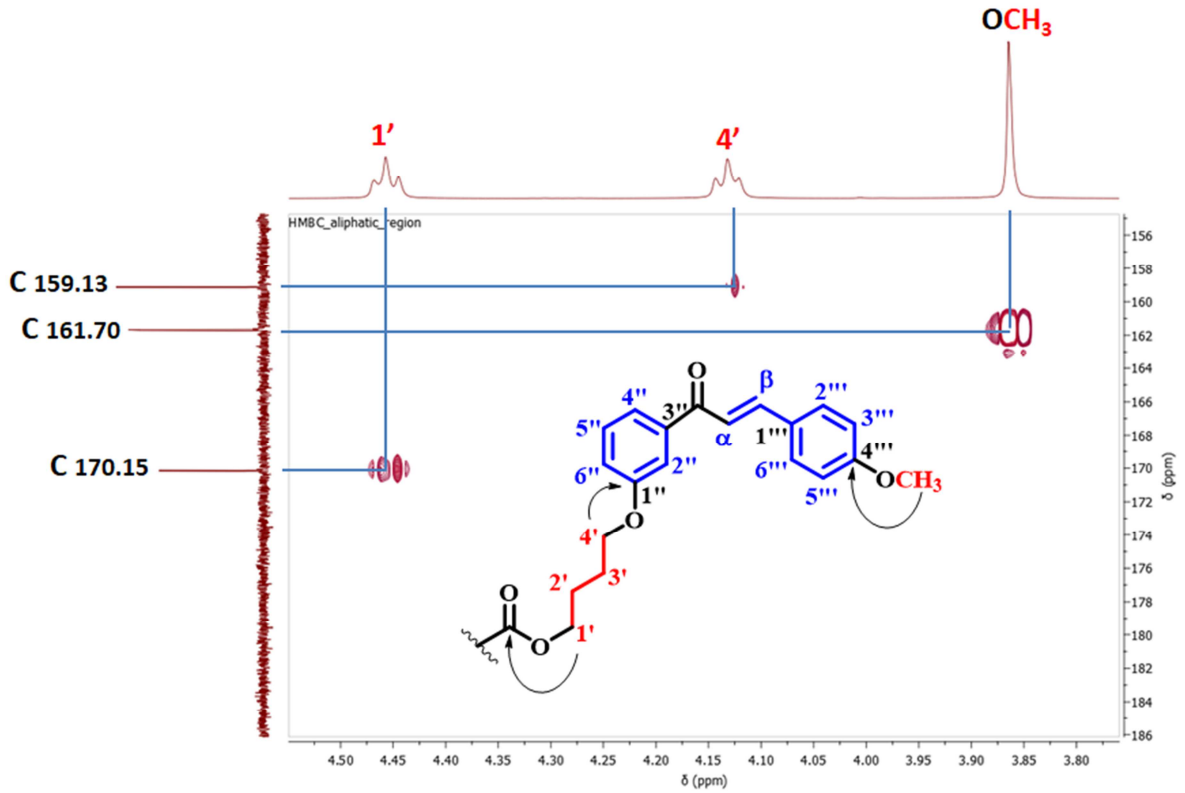

Figure S25. The important ^{1}H-^{13}C correlations of aliphatic protons in HMBC spectra of hybrid compound in $CDCl_3$

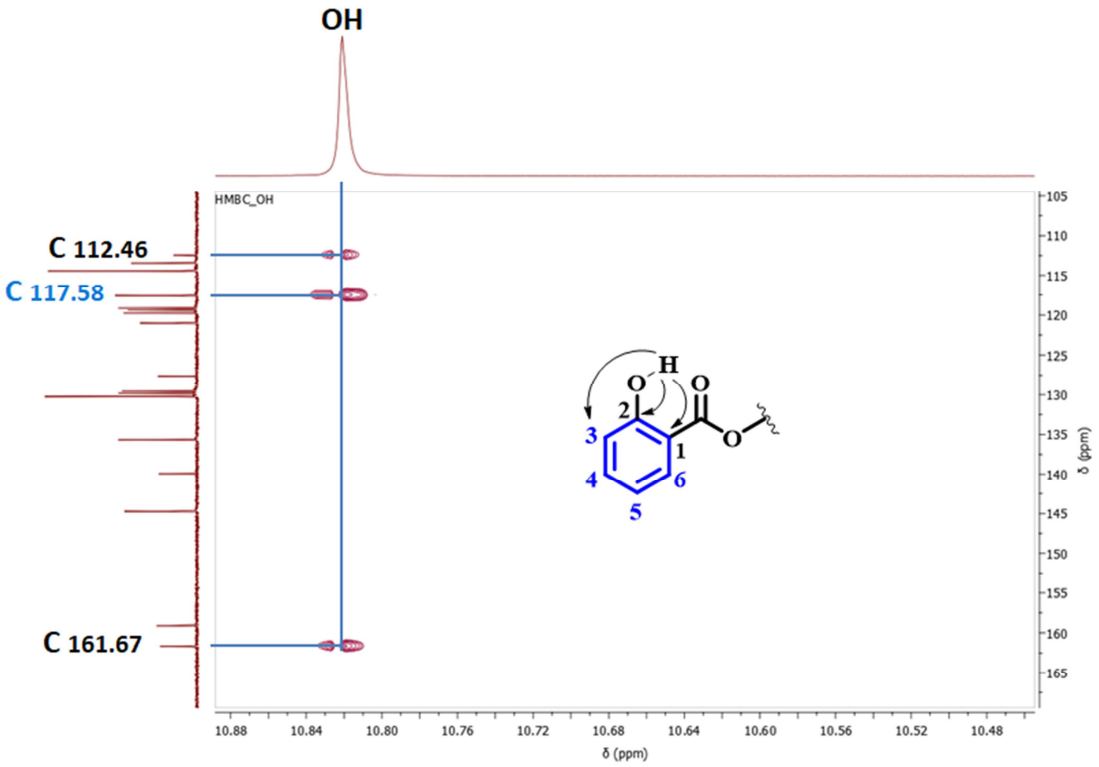

Figure S26. The important ^{1}H-^{13}C correlations of hydroxyl group in HMBC spectra of hybrid compound in $CDCl_3$

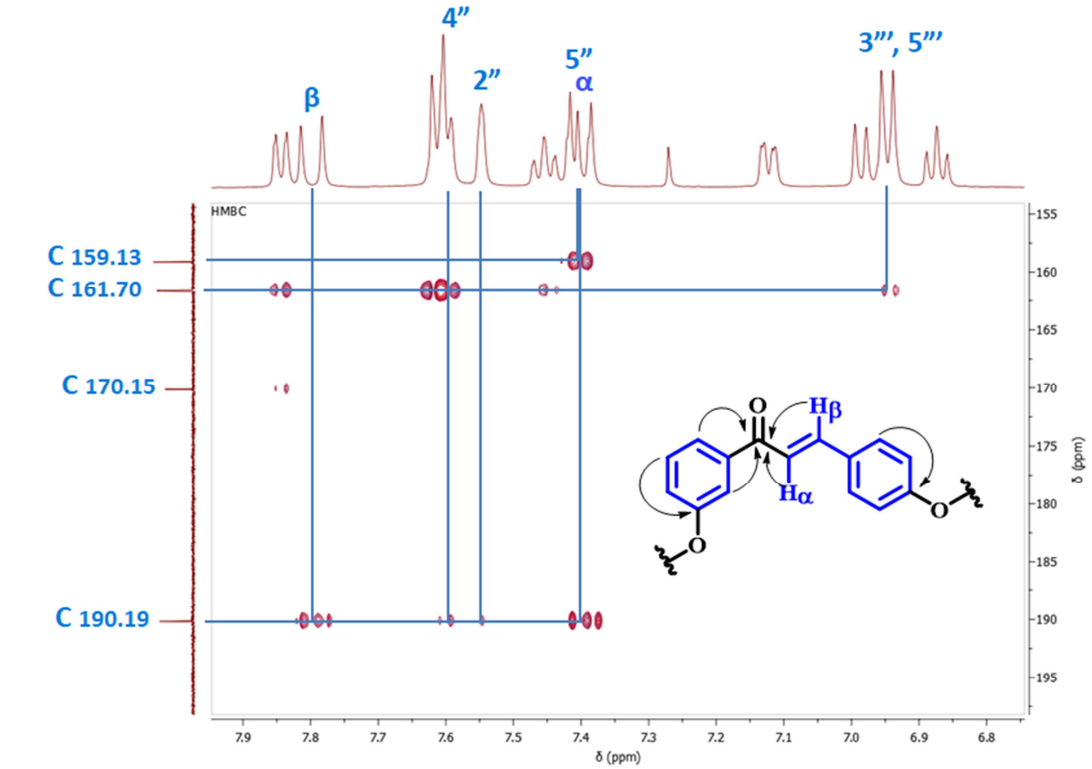

(a)

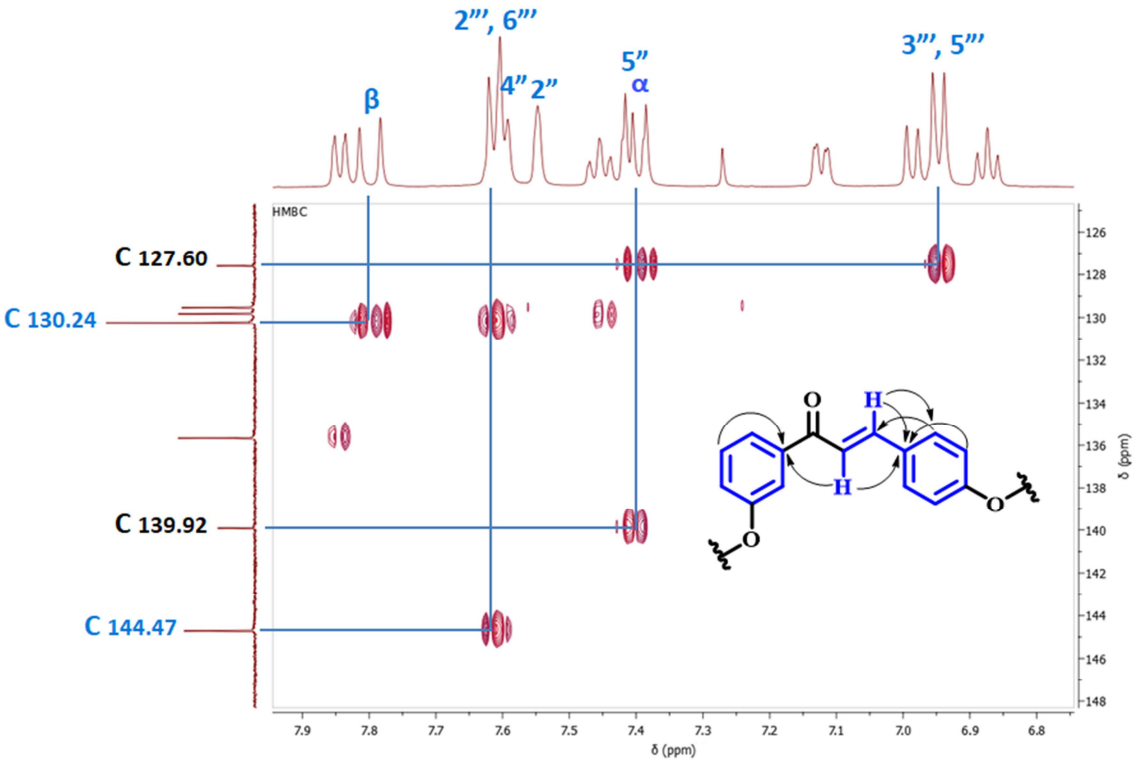

(b)

Figure S27. The important ^{1}H-^{13}C correlations of R" and R"' aromatic protons and *α*, β protons in HMBC spectra of hybrid compound in $CDCl_3$ (a) correlation with $C_{190.19}$ - $C_{159.13}$, (b) correlation with $C_{144.47}$ – $C_{127.60}$

Table S2. The result of docking protocol validation

Amino acid residues		Binding Similarity (%)	ΔG (kcal/mol)	RMSD (A°)
Co-crystalized Ligand	Re-docking Ligand			
Glu353	Glu353			
Arg394	Arg394			
Gly521	Gly521			
His524	His524			
Gly420	Gly420			
Glu419	Glu419			
Leu384	Leu384			
Thr347	Thr347			
Trp383	Trp383			
Leu349	Leu349			
Phe404	Phe404			
Asp351	Asp351			
Leu346	Leu346			
Met343	Met343	81,48	-9,0201	1,6606
Ala350	Ala350			
Leu387	Leu387			
Leu428	Leu428			
Leu391	Leu391			
Met388	Met388			
Ile424	Ile424			
Met421	Met421			
Leu525	Leu525			
-	Leu354			
-	Leu539			
-	Leu536			
-	Lys529			
-	Met522			

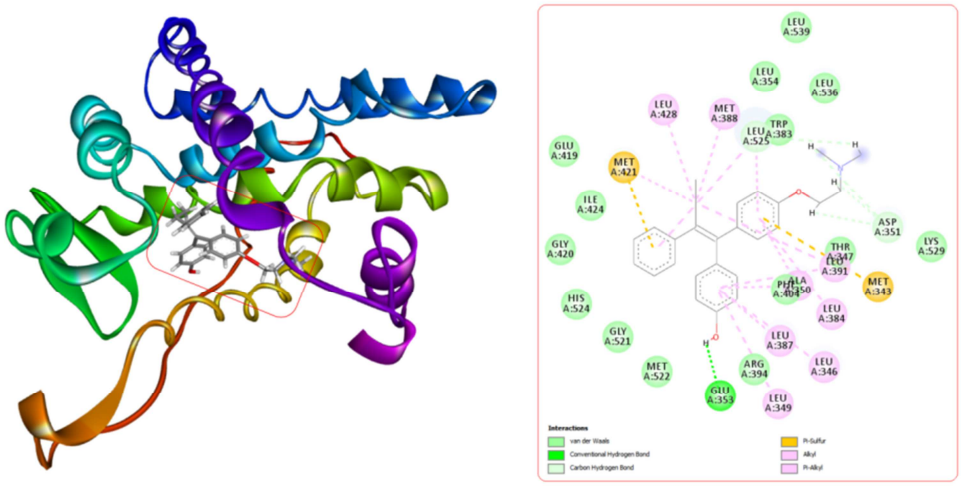

Figure S28. 3D and 2D binding poses of re-docked native ligand (4-OHT) to ER*α*

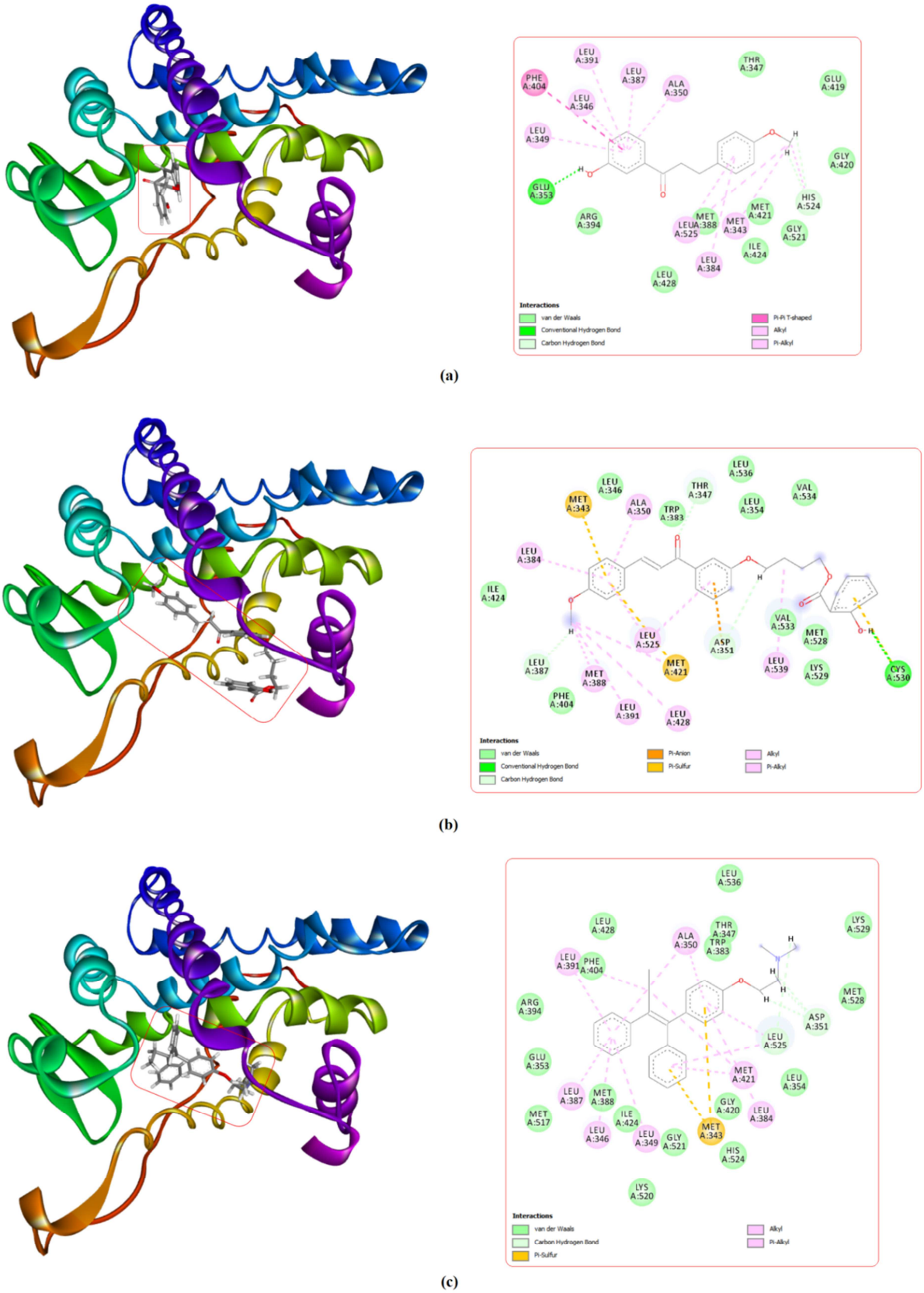

Figure S29. The 3D and 2D visualization of binding modes of docked compounds to ERα, (a) chalcone analogue, (b) title compound, (c) Tamoxifen

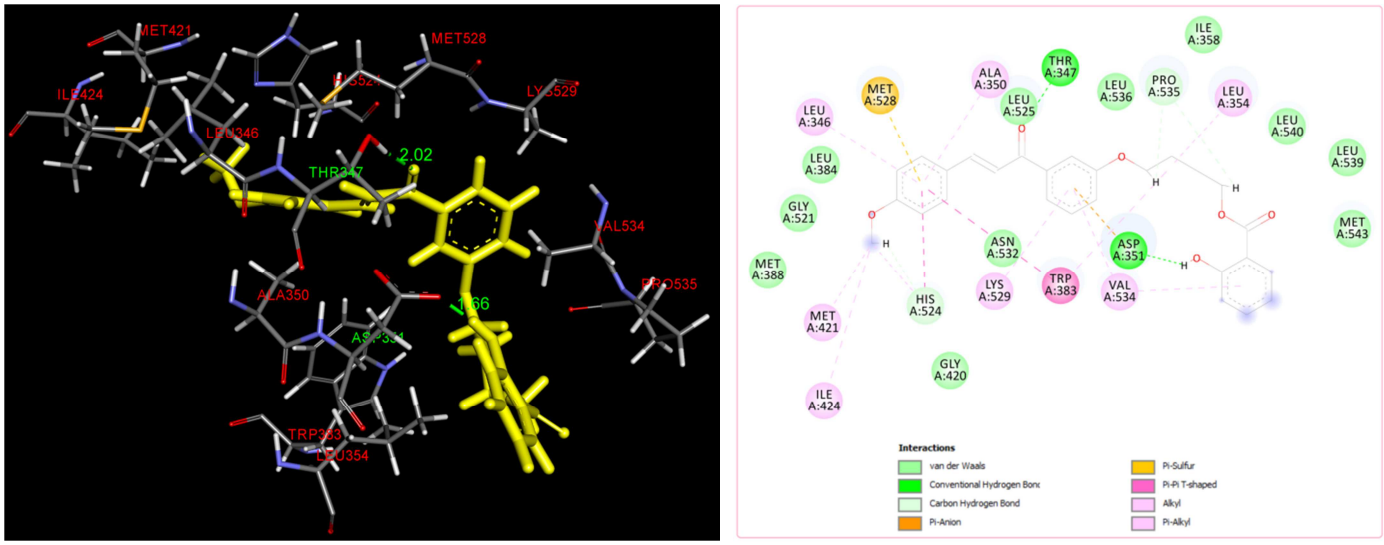

(a) **(b)**

Figure S30. The visualization of MD simulation result of the title compound using Discovery Studio 2020 Client (a) 3D visualization (b) 2D visualization